Sum Frequency Generation Imaging of Microcontact-Printed Monolayers Derived from Aliphatic Dithiocarboxylic Acids: Contrast Based on Terminal-Group Orientation

ARTICLE *in* THE JOURNAL OF PHYSICAL CHEMISTRY C · AUGUST 2007

Impact Factor: 4.77 · DOI: 10.1021/jp0746493

THE JOURNAL OF PHYSICAL CHEMISTRY C LETTERS

Published on Web 07/24/2007

Sum Frequency Generation Imaging of Microcontact-Printed Monolayers Derived from Aliphatic Dithiocarboxylic Acids: Contrast Based on Terminal-Group Orientation

Katherine Cimatu, H. Justin Moore, T. Randall Lee,* and Steven Baldelli*

Department of Chemistry, University of Houston, 4800 Calhoun Road, Houston, Texas 77204-5003

Received: June 15, 2007; In Final Form: July 6, 2007

The results of imaging μCP printed monolayers using sum frequency generation vibrational spectroscopy are presented, where the image contrast is based on the orientation of the terminal methyl groups. The printed regions contain thiols with 16 carbon atoms (even), and the backfilled regions contain 17 carbon atoms (odd). In the odd/even effect, the terminal group alternates its orientation as the number methylene group changes from even to odd. On the basis of this result, SFG imaging microscopy (SFGIM) is used to image the C16 and C17 regions where the difference is based on the orientation of the terminal methyl group. Furthermore, we compared the patterns formed by C16/C17 *n*-alkanethiols and C16/C17 aliphatic dithiocarboxylic acids. We find that the dithiocarboxylic acids form much-better patterns where the degree of mixing between the stamped and backfilled regions is reduced compared to the *n*-alkanethiols. Furthermore, this results shows that SFGIM is a useful technique to visualize monolayers based not only on the chemical functionality but also on the surface orientation of the adsorbates.

Introduction

Patterned surfaces are used for a myriad of applications in the fields of electronics, sensing, and medical diagnostics.[1,2] Microcontact printing (μCP) is a particularly convenient and versatile technique for creating patterned surfaces with selected terminal group functionality.[1,3−5] With μCP, the resolution of the pattern depends on several factors, including the precise nature of the molecules used in the stamping and backfilling steps.

Several methods have been developed that are able to image patterned surfaces based on chemical composition. In recent years, microspectroscopy with X-rays and atomic force microscopy have gained popularity in this area, particularly with regard to the imaging of electronic materials.[6−9] Molecular electronics that use organic thin films and monolayers that are spatially positioned in a device must be evaluated locally to gauge their performance at the molecular level. In particular, the density, orientation, and conformation of the molecules in the films may influence the conductivity, capacitance, rectification, and polarization of the device.[10] Therefore, experimental methods that have the capacity to investigate the integrity of the film at the molecular level with spatial resolution are very useful.

Often, self-assembled monolayers (SAMs) with various terminal functionalities are used to control the parameters of the film, such as the alignment of the molecules in a certain orientation or in a liquid crystalline phase. Field-effect transistors that depend on π-conjugation represent a particularly relevant example of this type of system.[7] Sum frequency generation, SFG, spectroscopy has the advantage of providing molecular specificity and surface sensitivity and is able to deduce orientation of molecules on the surface.[11,12] As an imaging technique, it is capable of providing spatial resolution on the order of 1 μm.[13,14]

This study demonstrates a new approach to the imaging of micropatterned surfaces by utilizing SFG spectroscopy to detect contrast arising solely from the different orientation of the terminal methyl group of patterned SAMs on gold having odd versus even chain lengths. The systematic variation in terminal-group orientation of SAMs is well-known[15] and is commonly referred to as the "odd−even" effect.[16] Previous research found that the odd−even effect for SAMs on gold derived from aliphatic dithiocarboxylic acids (i.e., $CH_3(CH_2)_nCS_2H$) is dramatically greater than that found for analogous films derived from simple *n*-alkanethiols (i.e., $CH_3(CH_2)_nSH$). The SFG-derived images in Figure 1 support this conclusion by showing dramatically enhanced contrast for the surfaces patterned with dithiocarboxylic acids, where the chains vary only by the length of a single methylene group.

Background

Sum Frequency Generation Spectroscopy. Sum frequency generation is a nonlinear vibrational spectroscopic technique that is used to detect molecules at the surface of a material. The technique involves overlapping two pulsed laser beams at the surface: one visible beam and one frequency tunable infrared beam, generating a third beam with a frequency that is the sum of the two input frequencies. When the infrared light is resonant with a surface vibrational mode, there is an increase in the nonlinear susceptibility, $\beta^{(2)}$, which is related to the SFG intensity, I_{SF}:

$$I_{SF} \propto \left|\sum_{JK} \chi^{(2)}_{I\,JK} E_J(\omega_{vis})\, E_K(\omega_{IR})\right|^2 \qquad (1)$$

where $\chi_{I\,JK}^{(2)}$ is the second-order nonlinear surface susceptibility and the $E(\omega)$ terms are light field amplitudes. The tensor, $\chi^{(2)}_{I\,JK}$, contains the information related to the interfacial structure. The

* Corresponding authors. E-mail: trlee@uh.edu; sbaldelli@uh.edu.

10.1021/jp0746493 CCC: $37.00

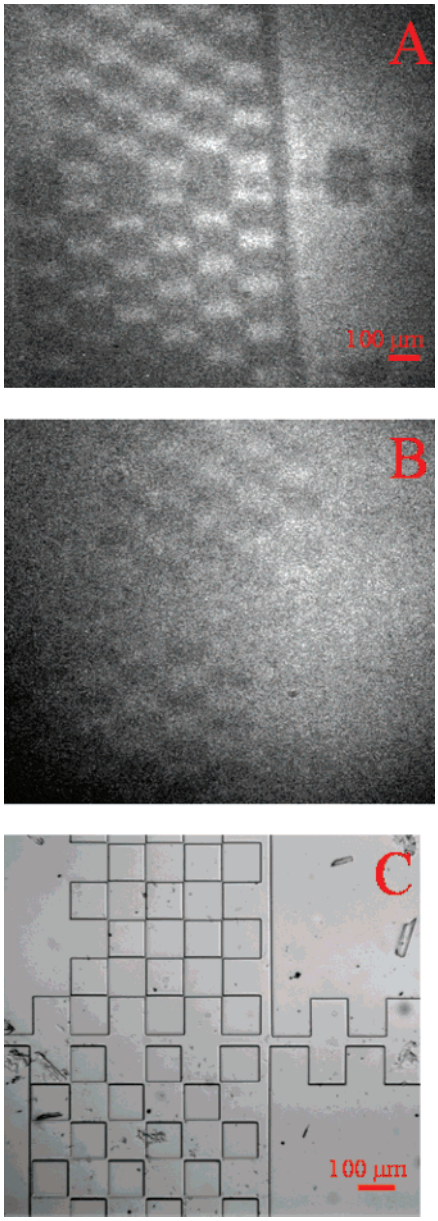

Figure 1. SFG image of C16/C17 printed/backfilled μCP-generated films: (A) aliphatic dithiocarboxylic acids, (B) *n*-alkanethiols, and (C) optical microscope image of PDMS stamp used in the μCP. Switching the molecules used for printing and backfilling gave the same contrast.

resonant portion contains the vibrational information of the molecules, $\chi_R^{(2)}$, whereas the nonresonant susceptibility is due primarily to the metal substrate, $\chi_{NR}^{(2)}$:

$$\chi^{(2)} = \chi_R^{(2)} + \chi_{NR}^{(2)} = \sum_q \frac{A_q}{\omega_{IR} - \omega_q + i\Gamma} + \chi_{NR}^{(2)} \qquad (2)$$

where ω_{IR} and ω_q are the infrared frequency and the resonant frequency of the qth vibrational mode, respectively. The damping factor of the vibration is Γ. The A_q term, line strength, contains information on the infrared and Raman transition moments:

$$\chi_R \propto N\langle\beta\rangle \qquad (3)$$

where N is the number of molecules generating signal, and $\langle\beta\rangle$ is the orientational averaged hyperpolarizability, which is the product of the infrared and Raman transition moments.

The orientation of the molecules at the surface is determined by a comparison of peak intensities of various vibrational modes.[17] For this analysis, molecular hyperpolarizibilities are calculated using bond additivity models and Raman depolarization ratios. Using eq 3, the molecular properties are related to the macroscopic surface susceptibility, $\chi^{(2)}$. The SFG experiment measures an effective surface susceptibility. Once this measurement is made, the experimental values are then related to the calculated values, and the orientation is determined.[18,19] This simple analysis assumes free rotation about the C_3 symmetry axis for methyl groups, an isotropic surface plane, and a δ-function distribution of tilt angles from the surface normal.[17,19−25]

Experimental Section

SFG Imaging. The recently developed technique of sum frequency generation imaging microscopy (SFGIM) provides images of the surface, where the contrast is based on the inherent vibrational spectrum of the adsorbed molecules.[14,26] In this experiment, SFG vibrational spectroscopy involves the spatial and temporal overlap of a fixed 1064-nm beam and a frequency-tunable IR beam that generates the SFG beam at a particular wavelength. The generated SFG signal is imaged onto a CCD camera.[14] All experiments were performed with the two input beams set to p polarization, where the output beam is necessarily p-polarized.[14] Images and spectra were obtained by continuously scanning the infrared frequency at 0.02 cm^{-1}/s and averaging the SFG signal over a 5-cm^{-1} interval. Each image acquisition was 5000 shots/image from 2800−3100 cm^{-1}. Local spectra were obtained by averaging a local region of the surface in the pattern with an approximate area of 60 × 60 μm^2 area. Vibrational spectra were acquired by extracting the signal intensity from the images and plotting it as a function of the infrared frequency using Origin software.[14]

Sample Preparation. The synthesis, characterization, and purification of alkanethiols and alkyldithiocarboxylic acids have been presented previously.[27,28] The gold substrate was rinsed with ethanol and dried with nitrogen gas. The PDMS stamp was saturated with the C16 dithiol in solution for 30−60 s, dried with nitrogen gas, and carefully placed onto the gold substrate for about 15 min. After the printing, the stamp was removed, and the substrate was rinsed with ethanol and dried with nitrogen gas. Then, the substrate containing the stamp features was placed into the C17 dithiol solution (backfilling) for 5 min, removed from solution, and dried under flowing N_2 gas.[29,30] Solution-deposited films prepared made by submerging gold films in 1 mM ethanolic solutions of the thiol for 18 h. After sample preparation, the μCP gold films were aligned in the SFG microscope for imaging/spectroscopy. All SFG experiments were performed in air at room temperature, 23 °C.

Results and Discussion

In a well-ordered alkanethiol monolayer on gold, the methylene chains typically adopt a predominantly all-trans conformation and are SFG-silent.[31] This consistent methylene conformation in the assembly does not give any SFG signal because it is considered to have inversion symmetry. SFG signal is generated only when molecules lack the inversion property where the molecules are both IR- and Raman-active. As the number of methylene groups in the alkyl chains alternates between odd and even, the terminal group also alternates in its orientation (i.e., tilt with respect to the surface normal).[16] This phenomenon is also accompanied by an alternation in surface energy and various interfacial properties such as wettability,[27,32]

TABLE 1: Intensity Values of CH_3 Peaks in the SFG Spectrum of SAMs on Gold Derived by Curve Fitting to Eq 1[a]

	n-alkanethiolate			*n*-alkane dithiocarboxylate		
solution	C16	C17	C16/C17	C16	C17	C16/C17
$I_{CH_3(sym)}$	7.1	5.5		9.3	6.6	
$I_{CH_3(asym)}$	6.8	11.6		7.1	16	
$R_{CH3} = I_{CH_3(sym)}/_{CH_3(asym)}$ pattern	1.0 (35°)	0.47(54°)	1.7	1.3(31°)	0.41(60°)	2.2
$I_{CH_3(sym)}$	17.9	10		5.6	1.9	
$I_{CH_3(asym)}$	21.5	21.2		7.2	13.7	
$R_{CH3} = I_{CH_3(sym)}/ I_{CH_3(sym)}$	0.83 (38°)	0.47(54°)	1.3	0.91(37°)	0.3(>65°)	3.0

[a] Values in parentheses are the estimated tilt angles from Figure 4.

friction,[33] and reactivity.[34] Furthermore, this effect is observed in the vibrational spectroscopy of SAMs by virtue of the "infrared dipole selection rule". This rule states that, on a metal surface, only the vibrational transitions with a normal mode component along the surface normal appear in the infrared or SFG spectra.[35,36]

The symmetric and asymmetric modes of the methyl groups are orthogonal. Consequently, as the C_3 axis of the CH_3 group tilts from 0° to 90° along the surface normal, the ratio $I_{CH_3(sym)}/I_{CH_3(asym)}$, which is denoted as R_{CH_3}, also changes.

The peak assignments for all of the shown spectra are the following: 2875, 2938, and 2965 cm^{-1}, which corresponds to the terminal methyl (CH_3) symmetric stretch, Fermi resonance, and the CH_3 asymmetric stretch, respectively. The other weak vibrational stretches present in the spectrum at 2850 and 2915 cm^{-1} are the methylene (CH_2) symmetric and asymmetric vibrational modes, presumably, due to gauche defects in the alkyl chains.[37−39]

As the terminal group changes orientation due to the odd−even effect, the dynamic dipole projection on the surface normal also changes.[35,40] Thus, both IR and SFG spectroscopy are highly effective probes of the odd−even effect on metal surfaces.[15]

There are three primary mechanisms for the contrast observed in the SFG images shown in Figure 1: (1) the degree of conformational order of the molecules in the monolayer, (2) the tilt angle of the molecules, and (3) the limited exchange/

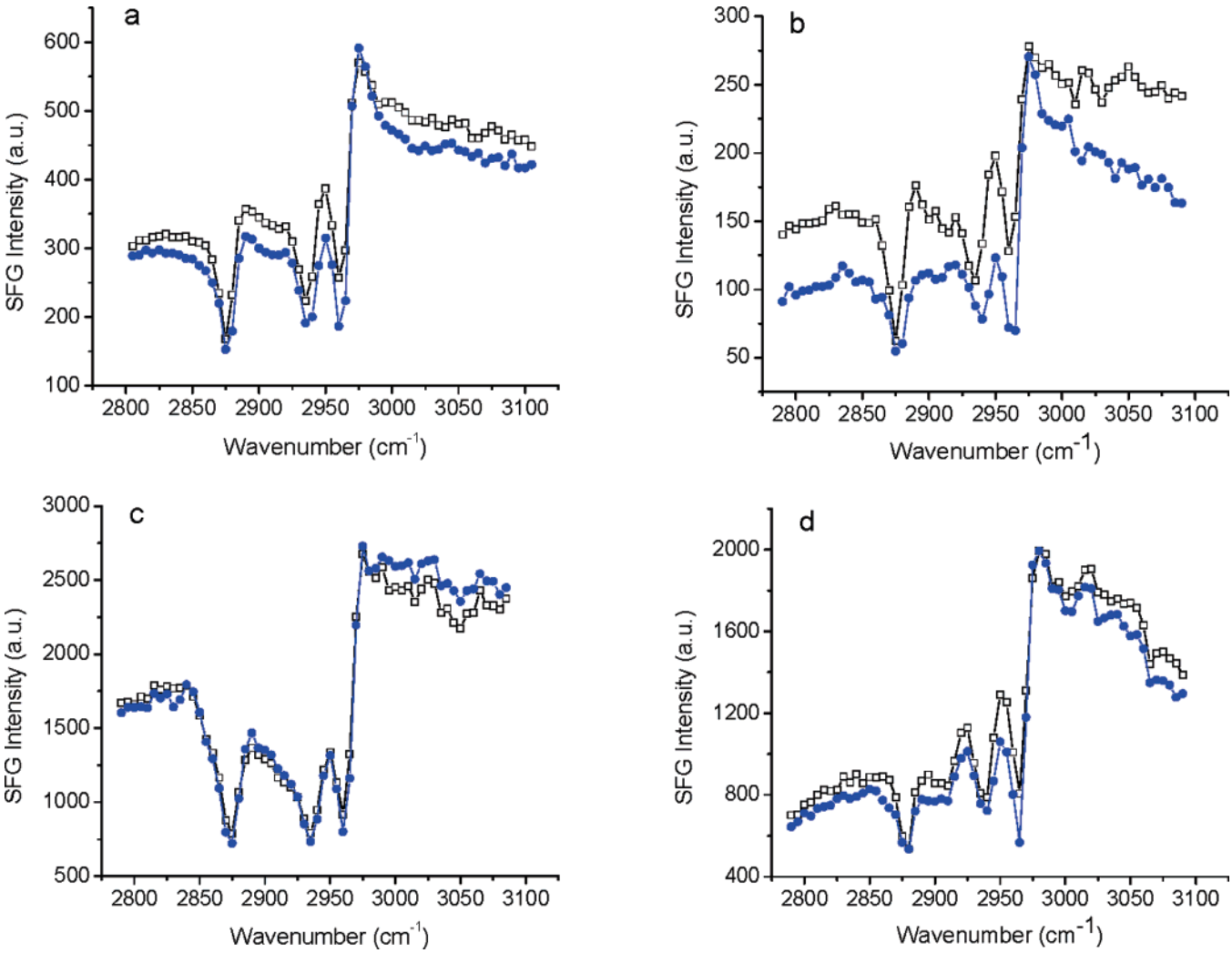

Figure 2. SFG spectra of (a) solution-deposited C16/C17 *n*-alkanethiol, (b) C16/C17 dithiocarboxylic acid, (c) C16/C17 *n*-alkanethiol patterned/backfilled, and (d) C16/C17 dithiocarboxylic acid patterned/backfilled. The SFG intensity scale is in arbitrary units without normalization. Black curves are for C16 and blue are for C17.

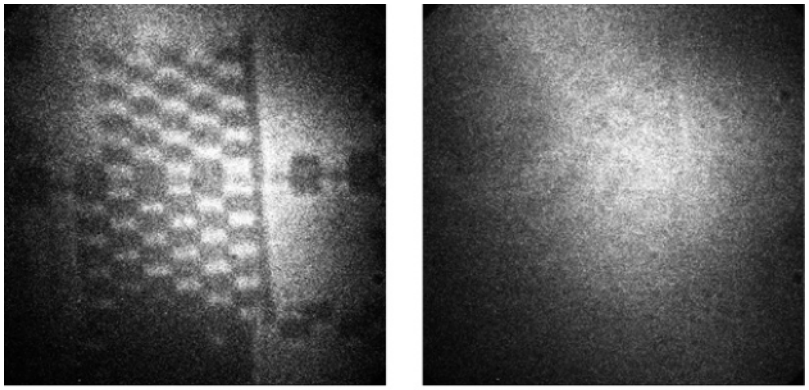

Figure 3. These are the SFG images of the C16/C17 dithiocarboxylic acid microcontact printed SAMs on gold where (A) an image taken at 2965 cm^{-1} and (B) an SFG image taken at 2875 cm^{-1}.

diffusion of molecules between stamped and backfilled regions on the surface during preparation.

In this experiment, the ratio between the symmetric and asymmetric CH_3 stretch (R_{CH_3}) alternates in magnitude as the chain length alternates between even and odd numbers of carbon atoms (C16/C17). The alternating magnitude of R_{CH_3} is one reason for the contrast observed in the SFG image because the bulk vibrational spectra are identical. Table 1 shows that the magnitude of $R_{CH_3}^{C16}/R_{CH_3}^{C17}$ for solution-deposited dithiocarboxylic acids (2.2) is greater than that for analogous normal alkanethiols (1.7). We attribute this difference in magnitude to a difference in orientation for these two classes of molecules[27,28] because no mixing is possible for these independent solution-deposited samples.

Figure 1A and B shows contrast based on orientation. These two images were taken at 2965 cm^{-1} where there is a resonance of the CH_3 asymmetric stretch vibrational mode. The dark areas, as seen, are from the backfilled region of the C17 molecules on the gold surface, and the bright areas are the regions where the C16 molecules are stamped.

The contrast is a result of a difference between the SFG signals of the odd/even thiol molecules at 2965 cm^{-1}. As the SFG intensity difference between both molecules becomes greater, the contrast observed in the images between the two regions increases. This difference in SFG signal is shown in Figure 2d.

The contrast depends on the orientation sensitivity of the vibrational mode. For example, the SFG taken at 2875 cm^{-1}, shown in Figure 3B, does not illustrate a significant contrast compared to the contrast shown by the SFG image taken at 2965 cm^{-1} in Figure 3A. Comparing these images with their corresponding spectra (in Figure 2d), the resonance peak of the CH_3 symmetric stretch (2875 cm^{-1}) is the same compared with difference observed at 2965 cm^{-1}. Thus, this change in contrast is inferred to be based on the change in orientation of the terminal methyl group of the chain (odd/even effect) as it affects the variation in the SFG intensity.

Quantitative comparison of the intensity ratio ($R_{CH_3}^{C16}/R_{CH_3}^{C17}$) for the solution-deposited monolayers relative to that for the μCP monolayers can then be a useful measure of the degree of mixing (during backfilling) between the C16/C17 molecules in the latter system. Table 1 shows that the magnitude of $R_{CH_3}^{C16}/R_{CH_3}^{C17}$ for μCP monolayers of dithiocarboxylic acids (3) is greater than the *n*-alkanethiols (1.3). A ratio of 1.0 would indicate complete mixing, and no contrast in the SFG image would be observed. Thus, the ratios obtained here suggest that the *n*-alkanethiolates are more labile than the aliphatic dithiocarboxylates in microcontact-printed films during the backfilling steps in solution.

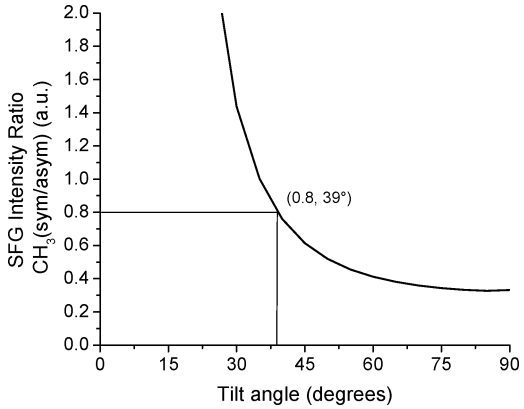

Figure 4. Plot of CH_3(sym/asym) intensity ratio vs tilt angle from the surface normal (θ). Shown is an example with a ratio of 0.8 that corresponds to a tilt angle of 39°.

The magnitude of R_{CH_3} can be used to estimate, qualitatively, the orientation of methyl groups with respect to the surface normal.[19,22,35,36,41] Likewise, the amplitude ratios were extracted via peak-fitting of the SFG spectra in Figure 2. The value of R_{CH_3} for solution-deposited C16-dithiocarboxylic acid was 1.3, which corresponds to a tilt orientation of 31° from surface normal; similarly, for C17-dithiocarboxylic acid, it was found to be 0.41 with a corresponding tilt angle of 60°. Estimation of the orientations for the SAMs derived from C16 and C17 *n*-alkanethiols gave 35° and 54°, respectively.[42,43] For the patterned monolayers, these values are markedly different: SAMs derived from the patterned C16/C17 dithiocarboxylic acid gave apparent methyl group tilts of 37° and >65°, respectively, whereas those derived from the patterned C16/C17 *n*-alkanethiol gave tilts of 39° and 54°, respectively. As noted above, the difference between the solution-deposited and patterned samples could be due to molecular mixing in the latter system.[14] Thus, as the degree of mixing between μCP and backfilled regions increases, the contrast in the SFG image decreases.

Contrast in SFG images is due to (1) fundamental differences in the SFG spectra of adsorbed molecules, (2) the degree of coverage, (3) incomplete mixing between various molecules, and (4) the conformational order and/or orientation of the molecules on the surface. On the basis of previous work[10] and the SFG imaging data obtained here, we conclude that dithiocarboxylic acids, when compared to *n*-alkanethiols, provide domains with greater contrast and boundaries with better edge resolution. The enhancements afforded by the dithiocarboxylic

acids likely arise from the chelating nature of the adsorbate,[27,28] which limits molecular diffusion and/or exchange during the backfilling process.[3,14,44] Finally, these studies have demonstrated a unique strategy for imaging micropatterned surfaces that relies solely on differences in terminal group orientation.

Acknowledgment. We thank the Texas Center for Superconductivity, the National Science Foundation (CHE-0650779 (SB) and ECS-0404308, DMR-0447588 (TRL)), and the Robert A. Welch Foundation (E-1320) for financial support.

References and Notes

(1) Gates, B. D.; Xu, Q.; Stewart, M.; Ryan, D.; Willson, C. G.; Whitesides, G. M. *Chem. Rev.* **2005**, *105*, 1171.
(2) Love, J. C.; Estroff, L. A.; Kriebel, J. K.; Nuzzo, R. G.; Whitesides, G. M. *Chem. Rev.* **2005**, *105*, 1103.
(3) Delamarche, E.; Schmid, H.; Bietsch, A.; Larsen, N. B.; Rothuizen, H.; Michel, B.; Biebuyck, H. *J. Phys. Chem. B* **1998**, *102*, 3324.
(4) Eberhardt, A. S.; Nyquist, R. M.; Parikh, A. N.; Zawodzinski, T.; Swanson, B. I. *Langmuir* **1999**, *15*, 1595.
(5) Wilbur, J. L.; Kumar, A.; Biebuyck, H.; Kim, E.; Whitesides, G. *Nanotechnology* **1996**, *7*, 452.
(6) Zharnikov, M.; Shaporenko, A.; Paul, A.; Golzhauser, A.; Scholl, A. *J. Phys. Chem. B* **2005**, *109*, 5168.
(7) Hu, W. S.; Tao, Y. T.; Hsu, Y. J.; Wei, D. H.; Wu, Y. S. *Langmuir* **2005**, *21*, 2260.
(8) Noy, A.; Frisbie, C. D.; Roznyai, L. F.; Wrighton, M. S.; Lieber, C. M. *J. Am. Chem. Soc.* **1995**, *117*, 7943.
(9) Wilbur, J. L.; Biebuyck, H. A.; MacDonald, J. C.; Whitesides, G. M. *Langmuir* **1995**, *11*, 825.
(10) Larsen, N. B.; Biebuyck, H.; Delamarche, E.; Michel, B. *J. Am. Chem. Soc.* **1997**, *119*, 3017.
(11) Huang, J. Y.; Shen, Y. R. In *Laser Spectroscopy and Photochemistry on Metal Surfaces*; Dai, H. L., Ho, W., Eds.; World Scientific: Singapore, 1995.
(12) Bain, C. D. *J. Chem. Soc. Faraday Trans* **1995**, *91*, 1281.
(13) Cimatu, K. A.; Baldelli, S. *J. Phys. Chem. C* **2007**, *111*, 7137.
(14) Cimatu, K. A.; Baldelli, S. *J. Phys. Chem. B* **2006**, *110*, 1807.
(15) Tao, Y. T.; Lee, M. T.; Chang, S. C. *J. Am. Chem. Soc.* **1993**, *115*, 9547.
(16) Tao, F.; Bernasek, S. L. *Chem. Rev.* **2007**, *107*, 1408.
(17) Wang, H. F.; Gan, W.; Lu, R.; Rao, Y.; Wu, B. H. *Int. Rev. Phys. Chem.* **2005**, *24*, 191.
(18) Lu, R.; Gan, W.; Wu, B. H.; Chen, H.; Wang, H. F. *J. Phys. Chem. B* **2004**, *108*, 7297.
(19) Lu, R.; Gan, W.; Wu, B. H.; Zhang, Z.; Guo, Y.; Wang, H. F. *J. Phys. Chem. B* **2005**, *109*, 14118.
(20) Gan, W.; Wu, B. H.; Chen, H.; Guo, Y.; Wang, H. F. *Chem. Phys. Lett.* **2005**, *406*, 467.
(21) Wang, J.; Clarke, M. L.; Chen, Z. *Anal. Chem.* **2004**, *76*, 2159.
(22) Hirose, C.; Akamatsu, N.; Domen, K. *J. Chem. Phys.* **1992**, *96*, 997.
(23) Hirose, C.; Akamatsu, N.; Domen, K. *Appl. Spectrosc.* **1992**, *46*, 1051.
(24) Hirose, C.; Yamamoto, H.; Akamatsu, N.; Domen, K. *J. Phys. Chem.* **1993**, *97*, 10064.
(25) Yamamoto, H.; Akamatsu, N.; Wada, A.; Hirose, C. *J. Electron Spectrosc. Relat. Phenom.* **1993**, *64/65*, 507.
(26) Cimatu, K. A.; Baldelli, S. *J. Am. Chem. Soc.* **2006**, *128*, 16016.
(27) Colorado, R.; Villazana, R. J.; Lee, T. R. *Langmuir* **1998**, *14*, 6337.
(28) Lee, T. C.; Hounihan, D. J.; Colorado, R.; Park, J. S.; Lee, T. R. *J. Phys. Chem. B* **2004**, *108*, 2648.
(29) Xia, Y.; Whitesides, G. M. *Angew. Chem., Int. Ed.* **1998**, *37*, 550.
(30) Xia, Y.; Whitesides, G. M. *Annu. Rev. Mater Sci.* **1998**, *28*, 53.
(31) Bain, C. D.; Davies, P. B.; Ong, T. H.; Ward, R. N. *Langmuir* **1991**, *7*, 1563.
(32) Laibinis, P. E.; Whitesides, G. M.; Allara, D. L.; Tao, Y. T.; Parikh, A. N.; Nuzzo, R. G. *J. Am. Chem. Soc.* **1991**, *113*, 7152.
(33) Carpick, R. W.; Salmeron, M. *Chem. Rev.* **1997**, *97*, 1163.
(34) Smith, D. L.; Wysocki, V. H.; Colorado, R., Jr.; Shmakova, O. E.; Graupe, M.; Lee, T. R. *Langmuir* **2002**, *18*, 3895.
(35) Greenler, R. G. *J. Chem. Phys.* **1966**, *44*, 310.
(36) Fan, J.; Trenary, M. *Langmuir* **1994**, *10*, 3649.
(37) MacPhail, R. A.; Strauss, H. L.; Snyder, R. G.; Elliger, C. A. *J. Phys. Chem.* **1984**, *88*, 334.
(38) Snyder, R. G. *J. Chem. Phys.* **1965**, *42*, 1744.
(39) Snyder, R. G.; Strauss, H. L.; Elliger, C. A. *J. Phys. Chem.* **1982**, *86*, 5145.
(40) Greenler, R. G. *J. Chem. Phys.* **1969**, *50*, 1963.
(41) Nishi, N.; Hobara, D.; Yamamoto, M.; Kakiuchi, T. *J. Chem. Phys.* **2003**, *118*, 1904.
(42) Zhang, H. P.; Romero, C. R.; Baldelli, S. *J. Phys. Chem. B* **2005**, *109*, 15520.
(43) Tanaka, Y.; Lin, S.; Aono, M.; Suzuki, T. *Appl. Phys. B* **1999**, *68*, 713.
(44) Kuhnke, K.; Hoffmann, D. M.; Wu, X. C.; Bittner, A. M.; Kern, K. *Appl. Phys. Lett.* **2003**, *83*, 3830.